11 Superconductivity and Magnetism

J. Hofer, H. Keller, R.I. Khasanov (since September 1999), M. Mali, P. Morf, J. Roos, A. Schilling, A. Shengelaya, M. Willemin (till September 1999), G.M. Zhao, S. Zech-Döttinger (since May 1999), C. Boekema (visiting scientist), V.A. Ivanshin (visiting scientist), B.I. Kochelaev (visiting scientist), T. Schneider (Titularprofessor), and K.A. Müller (Honorarprofessor)

in collaboration with:
ETH Zürich (K. Conder, J. Karpinski), PSI Villigen (E. Morenzoni), IBM Rüschlikon (C. Rossel), U. of Birmingham (E.M. Forgan, S.H. Lloyd, T.M. Riseman, T.J. Jackson, P.G. Kealey), U. of St. Andrews (S.L. Lee, F.Y. Ogrin, C. Ager), Institut Laue-Langevin, Grenoble (R. Cubitt), U. of Oxford (S.J. Blundell, B.W Lovett), RIKEN-RAL (F.L. Pratt), U. of Warwick (D.McK. Paul), U. of Tokyo (K. Kishio, T. Sasagawa), U. of Tsukuba, Tsukuba, Ibaraki, Japan (K. Kadowaki), U. of Maryland (R.L. Greene, T. Venkatesan, D.J. Kang, W. Prellier, M. Rajeswari), U. of Rome (A. Bianconi, N.L. Saini, A. Lanzara), U. of Berkeley (R.A. Fisher, N.E. Phillips), Los Alamos National Laboratory (M. Hundley, A. Lacerda), Argonne National Laboratory (U. Welp, W.K. Kwok, R.J. Olsson, G.W. Crabtree), Kazan State U., Russia (B.I. Kochelaev), U. of Belgrade, Yugoslavia (I.M. Savić), Institute of Low Temperature and Structure Research, Wroclaw, Poland (P.W. Klamut), Institute of Physics, Warsaw, Poland (A. Wisniewski), Northern Illinois U., DeKalb, USA (B. Dabrowski), Neurochirurgische Klinik, Stätisches Krankenhaus, Ingolstadt, Germany (A. Horowski).

11.1 Introduction

In the past year we have continued and extended our investigations of the magnetic and electronic properties of high-temperature superconductors (HTS) and related magnetic systems. In particular, we have performed extensive oxygen isotope ($^{16}O/^{18}O$) effect studies on various physical quantities (critical temperature, charge ordering temperature, spin glass temperature, in-plane penetration depth, EPR linewidth) in these systems in order to explore the role of lattice effects in these systems. Furthermore, we have continued our detailed study of the complex vortex state in HTS that we have started several years ago. Last year we have made an important extension of our solid state physics laboratory by incorporating a part of Prof. Brinkmann's former NMR/NQR laboratory, which is now under the supervision of the NMR/NQR specialists Dr. Roos and Dr. Mali. A major contribution to the strength of our work is the application of complementary experimental techniques such as muon spin rotation (μSR), small angle neutron scattering (SANS), NMR/NQR, electron paramagnetic resonance (EPR), together with bulk SQUID and torque magnetometry measurements, resistivity, and thermal measurements. This allows us to investigate the same physical problems on the same samples by means of different methods. The scientific goal of our research is not only to gain new insight on the basic understanding of high-temperature superconductivity, but also to contribute to a better understanding of vortex matter in these materials, which is of fundamental importance for technical applications.

11.2 Studies of oxygen isotope effects

11.2.1 Oxygen isotope effects in manganites

The magnetic properties of the manganite perovskites $Re_{1-x}A_xMnO_3$ (Re = a rare-earth element, and A = a divalent element) have attracted renewed interest because of the observation of colossal magnetoresistance (CMR) in thin films of these materials [1, 2]. Despite

of tremendous experimental efforts [3], the basic physics and the microscopic mechanism for CMR in these materials remain controversial [4, 5, 6].

In order to discriminate among those different models, we study the oxygen isotope effect on the transport properties of high-quality epitaxial thin films of $La_{0.75}Ca_{0.25}MnO_3$ and $Nd_{0.7}Sr_{0.3}MnO_3$. The intrinsic resistivity of these compounds shows a strong dependence on the oxygen isotope mass in both the paramagnetic and the ferromagnetic state (see Fig. 11.1).

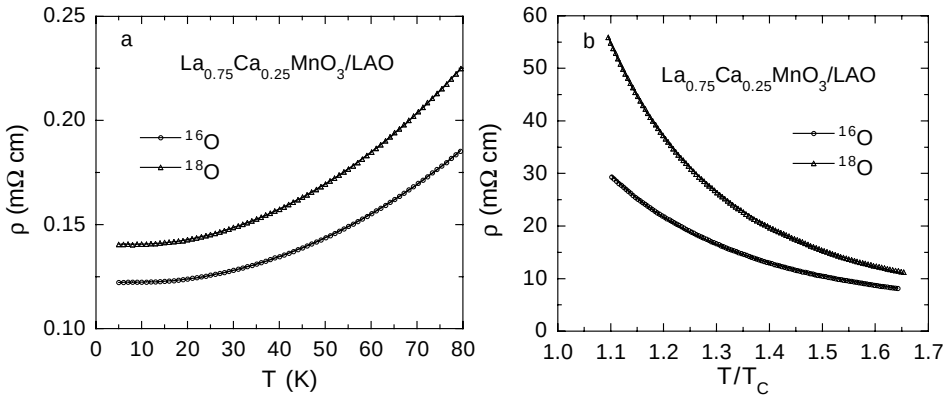

Figure 11.1: *Temperature dependence of the resistivity in the ferromagnetic (a) and paramagnetic (b) state in the oxygen-isotope exchanged thin film of* $La_{0.75}Ca_{0.25}MnO_3$. *The solid lines are the fitted curves.*

In the ferromagnetic state, the data can be perfectly fit by

$$\rho(T) = \rho_0 + BT^{4.5} + C\omega_s / \sinh^2(\hbar\omega_s/2k_BT).$$

Here ρ_o is the residual resistivity, the second term arises from 2-magnon scattering, and the third term is associated with small-polaron coherent motion which involves a relaxation due to a soft optical phonon mode [7]. Such a soft mode is related to the tilt/rotation of the oxygen octahedra, and has a low frequency ($\hbar\omega_s/k_B \sim 80$ K). Both ρ_o and the coefficient C should be proportional to the effective carrier mass m^*, and depend strongly on the oxygen isotope mass if the carriers in the ferromagnetic state is of small polaron type. Indeed, we find that both quantities increase by 15(3)% upon replacing ^{16}O with ^{18}O isotope. The result provides first experimental evidence for the presence of small polaronic carriers and their metallic conduction in the low temperature ferromagnetic state, and is in quantitative agreement with a CMR theory proposed by Alexandrov and Bratkovsky [6].

In the paramagnetic state, the data can be well fit by [8]

$$\rho = \frac{A}{\sqrt{T}} \exp(E_\rho/k_BT),$$

where $A = (ah/e^2\sqrt{k_B})(1.05W_p)^{1.5}/\hbar\omega_o$, W_p is the polaron bandwidth, $E_\rho = E_a + \Delta/2$, Δ is the bipolaron binding energy, E_a is the activation energy of small polaron hopping mobility. The quantity A should strongly depend on the isotope mass, and Δ is also isotope-mass dependent according to a theoretical model [6]. It is striking that, upon replacing ^{16}O with ^{18}O isotope, the parameter A decreases by 35(5)%, and E_ρ increases by 13.2(5) meV. The result is in quantitative agreement with the CMR theory by Alexandrov and Bratkovsky [6].

11.2.2 Oxygen isotope effects in cuprates

a) Charge-stripe ordering in $La_{1.94}Sr_{0.06}CuO_4$

One of the outstanding features in the high-temperature copper oxide superconductors is the formation of alternating spin and charge stripes below a characteristic temperature [9, 10]. Such a stripe phase is believed to be important to the understanding of the pairing mechanism of high-temperature superconductivity [11]. However, the microscopic origin of the stripe phase is still highly debated. It could be caused by purely electronic interactions and/or by a strong electron-phonon interaction.

Although there is increasing experimental evidence for the presence of a strong electron-phonon interaction in the cuprate superconductors, it is not clear whether this interaction is relevant for the formation of the stripe phase. For the colossal magnetoresistive manganites, a strong electron-phonon interaction plays an important role in the formation of the Jahn-Teller paired stripes (or charge ordering), as shown by a very large oxygen-isotope shift of the charge-ordering temperature in both $Nd_{0.5}Sr_{0.5}MnO_3$ and $La_{0.5}Ca_{0.5}MnO_3$ systems [12]. Therefore it is natural to expect that the stripe formation temperature in cuprates should also depend on the oxygen-isotope mass if lattice vibrations are strongly coupled to the charge carriers.

The x-ray absorption near edge spectroscopy (XANES) is a powerful technique to probe the local structure conformations for a system. There are two characteristic peaks in the XANES spectra of the cuprates, which characterize the local structures within and out of the CuO_2 planes. A parameter R is defined as $R = (\beta_1 - \alpha_1)/(\beta_1 + \alpha_1)$, where β_1 and α_1 are the intensities of two characteristic peaks observed by XANES. When acharge-stripe ordering takes place, a change in the local structures leads to a sudden increase in R below the charge-stripe formation temperature T^*. The identification of T^* by XANES has been tested in an extensively studied compound $La_{1.875}Ba_{0.125}CuO_4$ [13].

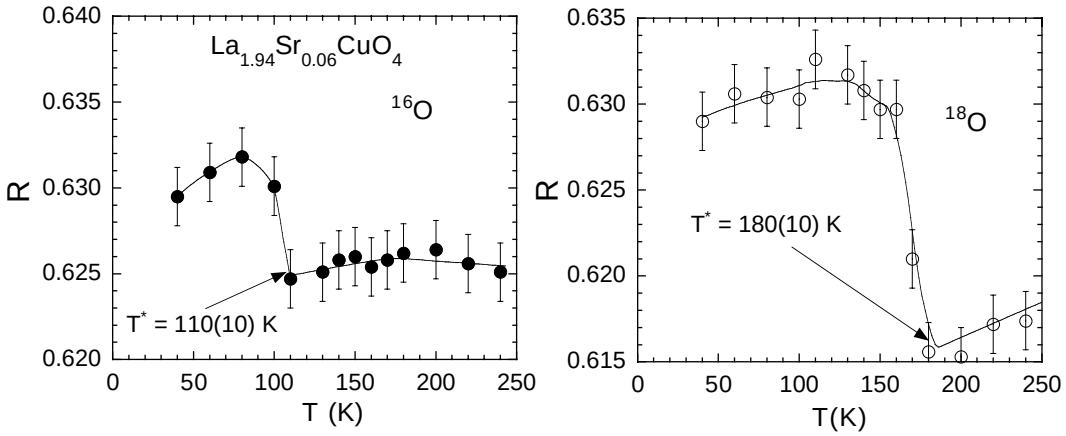

Figure 11.2: *Oxygen isotope effect on charge-stripe ordering temperature T^* in $La_{1.94}Sr_{0.06}CuO_4$, as determined from XANES peak intensity ratio R (see text).*

In Fig. 11.2, we show the temperature dependence of the parameter R for the oxygen isotope exchanged $La_{1.94}Sr_{0.06}CuO_4$. From the figure, one can clearly see that, upon replacing ^{16}O with ^{18}O, the stripe formation temperature T^* in this cuprate increases from about 110 K to 180 K. Such a huge oxygen isotope shift of T^* indicates that a strong electron-phonon interaction is likely to be involved in both the charge-stripe formation and the occurrence of high-temperature superconductivity.

b) Spin glass transition

There is increasing evidence that a strong electron-phonon coupling is present in the cuprates, which may lead to the formation of polarons (bare charge carriers accompanied by local lattice distortions). Several independent experiments have demonstrated that superconductivity and the underlying lattice vibrations are intimately linked. On the other hand, little is known about the influence of the electron-phonon interaction on magnetism in the cuprates. Conventional theories of magnetism neglect atomic vibrations; the atoms are generally considered as infinitely heavy and static in theoretical descriptions of magnetic phenomena, so there should be no isotope effect on magnetism. However, if charge carriers are polaronic, i.e., nuclear and electronic motions are no longer decoupled, one might expect isotope effects on magnetic properties. The question is whether such an isotope effect exists in the cuprates.

In order to answer this question we performed studies of the oxygen-isotope effect on the low temperature magnetism in $La_{2-x}Sr_xCu_{1-z}Mn_zO_4$ ($x = 0.03, 0.05$; $z = 0, 0.02$) using the zero-field μSR technique [14]. These samples are in the so-called cluster spin glass regime. The pair of samples with different oxygen isotopes ^{16}O and ^{18}O were mounted on the two sides of the sample holder. This allows one to switch between the two isotope samples by rotating the sample holder without removing it from the cryostat, so the two isotope samples can be investigated at the same experimental conditions.

At low temperatures in all studied samples we observed damped oscillations due to muon-spin precession in local magnetic fields. A clear oscillation observed in ZF-μSR spectra implies that the muons sense a well defined internal magnetic field, in agreement with previous μSR measurements [15].

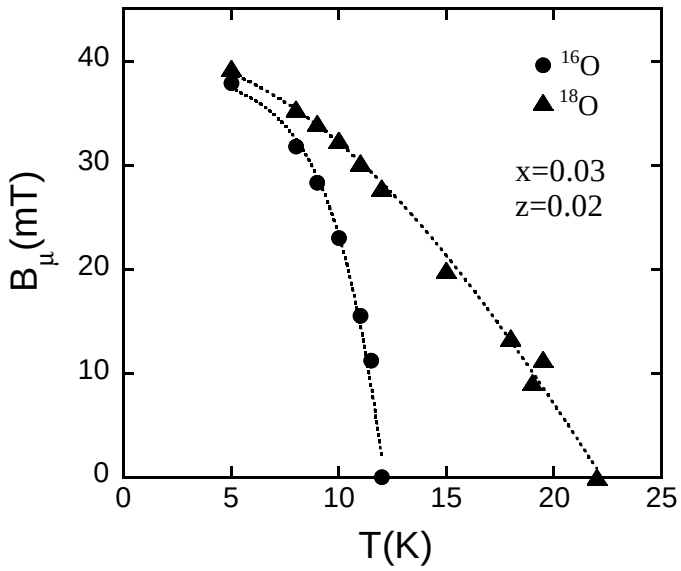

Figure 11.3: *Temperature dependence of the internal magnetic field at the muon site B_μ for the ^{16}O and ^{18}O samples of $La_{1.97}Sr_{0.03}Cu_{0.98}Mn_{0.02}O_4$. Dotted lines are guides to the eye.*

Fig. 11.3 shows the internal magnetic field B_μ for the two oxygen isotope (^{16}O and ^{18}O) samples ($x = 0.03$, $z = 0.02$) as a function of temperature. One can see that the spin glass freezing temperature T_g is strongly isotope dependent. The T_g of the ^{18}O sample is 10 K higher than that of the ^{16}O sample. This results in a huge value of the oxygen isotope exponent for the spin glass freezing temperature: $\alpha_{T_g} = -d\ln T_g / d\ln M = -6.0(7)$, which is the largest *negative* oxygen isotope exponent ever measured for any phase transition temperature. These novel isotope effects clearly demonstrate a strong effect of lattice vibrations on magnetism in cuprates which can be explained taking into account the polaronic nature of the charge carriers.

c) Magnetic penetration depth

Most oxygen isotope effect (OIE) studies performed on HTS were carried out on powder samples so far [16, 17]. In the small grains of these samples an almost complete oxygen isotope exchange by diffusion can be achieved. However, due to the strongly anisotropic nature of HTS (expressed in terms of the effective mass anisotropy $\gamma = \sqrt{m_c^*/m_{ab}^*}$) isotope experiments on single crystals are advantageous. Magnetic OIE studies on $La_{2-x}Sr_xCuO_4$ microcrystals with a mass of only 3 - 12 μg were performed during the last year [18]. SQUID magnetometry, which is the most commonly used technique for investigating magnetic properties of superconductors, is not sensitive enough for measuring such small samples. Therefore, a highly sensitive miniaturized torque magnetometer [19] (see also Annual Report 96/97) was used to perform all magnetic measurements. This device measures the magnetic torque $\vec{\tau} = \vec{m} \times \vec{B_a}$ acting on the magnetic moment $\vec{m}$ of a HTS single crystal in an applied magnetic field $\vec{B_a}$.

Temperature-dependent torque measurements were performed at a fixed magnetic field $B_a = 0.1$ T and at an angle $\delta = 45°$ of $\vec{B_a}$ with respect to the c-axis of the sample. An example of these measurements carried out on an underdoped $La_{2-x}Sr_xCuO_4$ microcrystal (mass ~ 3 μg) with $x = 0.086$ is displayed in Fig. 11.4a. Clearly, an OIE on the critical temperature T_c is observed. The excellent reproducibility of the oxygen exchange procedure as demonstrated by the back-exchanged data (crosses) gives evidence that a complete isotope exchange by diffusion was achieved in this tiny single crystal.

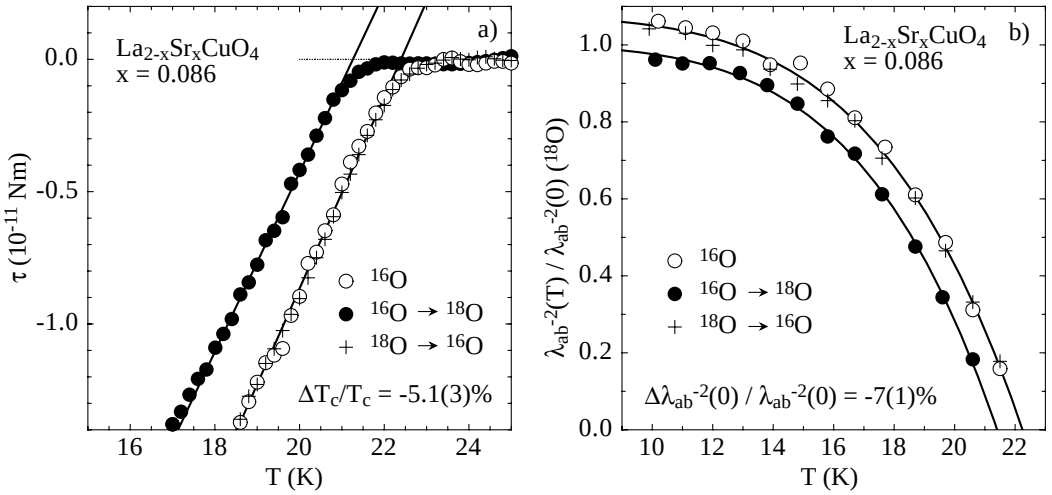

Figure 11.4: *a) Magnetic torque τ versus temperature for $La_{2-x}Sr_xCuO_4$ with $x = 0.086$, showing the OIE on T_c. The reproducibility of the exchange procedure, as checked by the back-exchange (crosses), demonstrates a complete isotope exchange. b) Normalized in-plane penetration depth $\lambda_{ab}^{-2}(T)/\lambda_{ab}^{-2}(0)(^{18}O)$ for $La_{2-x}Sr_xCuO_4$ with $x = 0.086$. An OIE not only on T_c but also on $\lambda_{ab}^{-2}(T)$ is clearly seen.*

The in-plane penetration depth $\lambda_{ab}(T)$ was extracted from field-dependent torque measurements performed at different temperatures $0.5T_c < T < T_c$ at an angle $\delta = 45°$. $\lambda_{ab}(T)$ was determined from the logarithmic field dependence of $\tau/B_a \propto m$, characteristic for HTS in small fields [20, 21]. The normalized penetration depth $\lambda_{ab}^{-2}(T)/\lambda_{ab}^{-2}(0)(^{18}O)$ for the $^{16}O/^{18}O$ exchanged $La_{2-x}Sr_xCuO_4$ microcrystal with $x = 0.086$ is shown in Fig. 11.4b. Again, the OIE on T_c is clearly seen. Furthermore, a systematic shift of $\lambda_{ab}^{-2}(T)$ upon replacing ^{16}O by ^{18}O is observed. The value $\lambda_{ab}^{-2}(0)$ is determined by extrapolating the data to low temper-

atures, using the power law $\lambda_{ab}^{-2}(T) = \lambda_{ab}^{-2}(0)(1-(T/T_c)^n)$ (solid lines). An oxygen isotope shift of $-7(1)\%$ is found. Many different experiments show that the change of the charge carrier density n_s during the oxygen isotope exchange procedure is negligible [17]. The excellent reproducibility of the isotope exchange gives further evidence that n_s is unaltered. We thus conclude that the observed OIE on $\lambda_{ab}^{-2}(0) \propto n_s/m_{ab}^*$ is due to an OIE on the effective in-plane mass m_{ab}^* of the charge carriers. This implies that lattice vibrations play an important role in the occurrence of HTS. A bipolaronic model of HTS [22] can quantitatively explain the OIE on m_{ab}^*.

d) EPR relaxation

A number of experiments on HTS suggest the possible existence of two quasiparticles: a heavy Jahn-Teller (JT) type polaron and a light fermion [23]. In the present study we performed electron paramagnetic resonance (EPR) experiments on $La_{2-x}Sr_xCuO_4$ ($0 \leq x \leq 0.20$) with different oxygen isotopes ^{16}O and ^{18}O. In order to observe the EPR signal, $La_{2-x}Sr_xCuO_4$ was doped with 2% of Mn^{2+} ions which replace the Cu ions in the copper-oxygen layer and serve as an EPR probe. The temperature dependence of the EPR linewidth was studied from 4 K to 300 K. Fig. 11.5 shows the EPR line observed in a x=0.03 sample with different

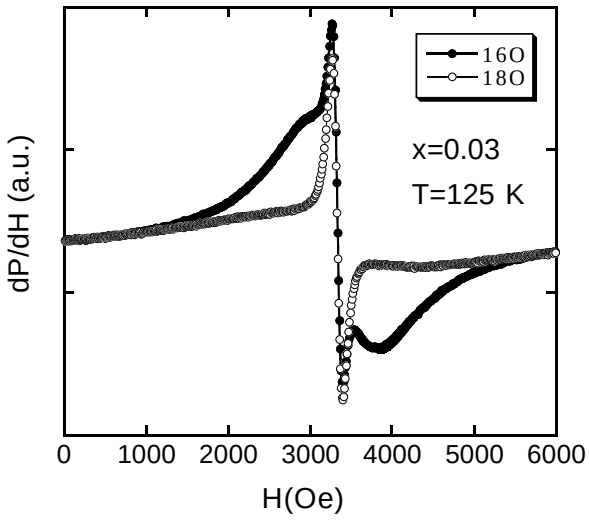

Figure 11.5: *EPR signal of ^{16}O and ^{18}O samples of $La_{1.97}Sr_{0.03}Cu_{0.98}Mn_{0.02}O_4$ measured at T=125 K under identical experimental conditions. The solid lines represent the best fits using a sum of two Lorentzian components with different linewidths: a narrow and a broad one.*

oxygen isotopes. First of all one should note that at this particular Sr concentration the EPR spectrum consists of two lines. We found that it can be well fitted by a sum of two Lorentzian components with different linewidths: a narrow and a broad one. One can see from Fig. 11.5 that the narrow line is not affected by the oxygen isotope substitution, while the linewidth of the broad signal exhibits a huge isotope effect. We found that at low temperatures the linewidth of the ^{18}O sample is almost twice larger than the one of the ^{16}O sample. We assign the narrow line to the light carriers and the broad one to the heavy polarons. With increasing doping the two EPR lines merge into a single EPR line, and the isotope effect on the linewidth gradually decreases towards optimum doping. Our results strongly suggest the presence of two quasiparticles in underdoped $La_{2-x}Sr_xCuO_4$. Moreover, the isotope effect observed on the EPR signal provides the first *microscopic* evidence for polaronic charge carriers in cuprate superconductors [24].

11.3 NMR/NQR studies of charge fluctuations in cuprates

One of the central issues in understanding cuprate-based HTS has been to determine in the CuO_2 planes the minimal number of electronic degrees of freedom which are necessary to describe the physics at the atomic scale. According to the so-called *single-spin fluid model* [25] only *one* spin degree of freedom would be necessary to describe the low-energy dynamics of the electronic system in the normal state of the HTS. However, as was discussed by various authors [26], this model might be an oversimplification.

This problem can be addressed by nuclear magnetic resonance (NMR) which probes the low-energy excitations of the HTS electronic system and separately provides information about the electronic structure of copper and oxygen. To examine whether a charge degree of freedom is present in the electronic dynamics, we studied the spin-lattice relaxation (SLR) of plane oxygen in $YBa_2Cu_4O_8$ by employing a recently developed double irradiation technique [27]. In this experiment two ^{17}O NMR spectra are compared, one obtained by starting from thermal equilibrium (standard spin-echo experiment), the other obtained by dynamic saturation of the $-1/2 \leftrightarrow 1/2$ NMR transition of the plane oxygen nuclear spin system. Charge fluctuations cause a quadrupolar contribution to the magnetically dominated SLR and this contribution, if present, will lead to an enhancement of the NMR line intensity at the inner satellite position during dynamic saturation.

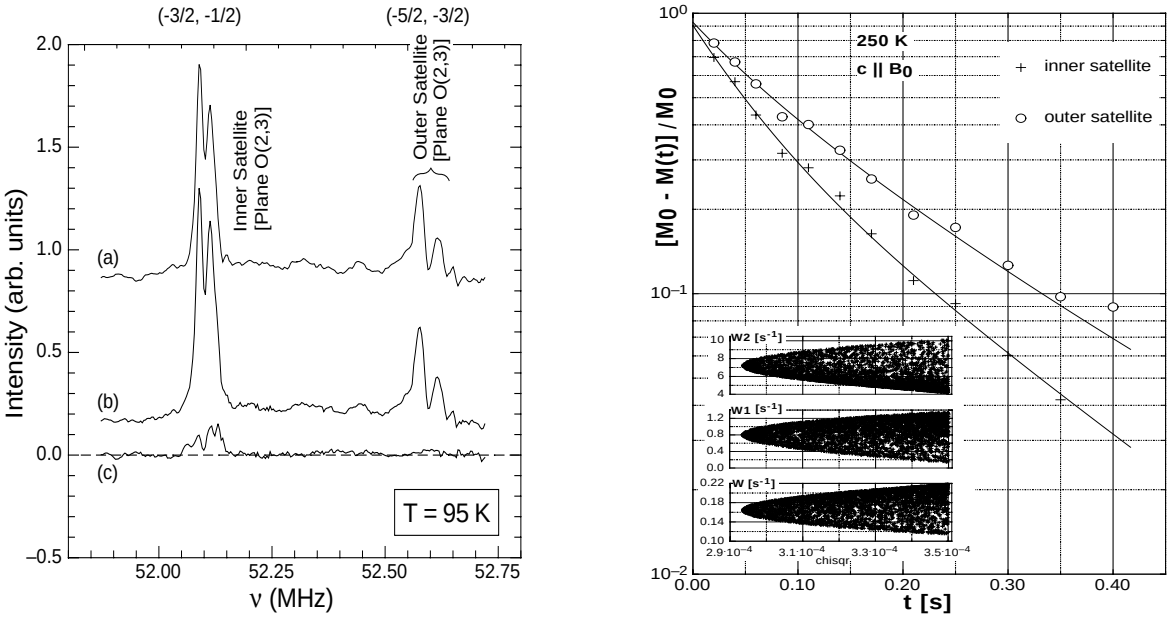

Figure 11.6: *Left:* ^{17}O *central transition and high-frequency satellites of plane oxygen: (a) in a standard spin-echo experiment, (b) after dynamic saturation of the* $(-1/2, 1/2)$ *transition. (c) Difference of spectrum (b) and (a). Right: The best simultaneous fit of the multi-exponential magnetization recovery* $M(t)$ *as a function of* W, W_1, W_2 *to experimental data for inner and outer satellite. Inset: sets of* W, W_1, W_2 *values plotted versus* χ^2*.*

The left part of Fig. 11.6 shows a series of such spectra measured in oriented powder at $T = 95$ K with the magnetic field applied along the c axis. The remaining intensity at the inner satellite position in the difference spectrum clearly demonstrates that the SLR at the plane oxygen site in $YBa_2Cu_4O_8$ is not only driven by spin but also by charge fluctuations. We could show [28] that the origin of this low-frequency charge fluctuations is linked neither directly to phonons nor to electron-like quasiparticles. We can further rule out defect motion

of ions. Therefore, the substantial quadrupolar relaxation we observe has to arise either from strongly *correlated* quasiparticles as proposed by different theoretical models [29], or from very strong electron-phonon interactions that could lead to heavy polaronic-like quasiparticles [22, 30].

In addition, $YBa_2Cu_4O_8$ contains double Cu-O chains that present a good example of a quasi-one-dimensional (1D) electronic conductor, where non-Fermi liquid behavior due to strong electron-electron interaction is expected. If probed by NMR or nuclear quadrupole resonance (NQR) the chains do not exhibit simple metallic behavior. Instead, the chain Cu Knight shift varies linearly with temperature, T, rather than remaining constant, and the Cu SLR rate increases with T^3 [31] rather than being linearly dependent on T.

As shown in ref. [31] apex oxygen reflects the electronic behavior of the chain. Its magnetic shift scales with the chain Cu magnetic shift, but not with that of the plane Cu; thus indicating that the 2p apex orbitals only slightly overlap with the plane Cu 3d orbitals. On the other hand, SLR of apex oxygen scales neither with chain Cu nor with plane Cu but with the quadrupolar part of the chain Cu relaxation [31]. This implies that electric field gradient (EFG) fluctuations, presumably induced by charged quasi-particles in the chain, are responsible for the apex oxygen relaxation. Surprisingly, the two relaxation contributions of chain Cu, namely the charge induced quadrupolar and the spin induced magnetic relaxation, do not have the same temperature dependence. This fact points to separate dynamics for charge and spin that could, for instance, originate from a spin-charge separation expected in 1D conductors. Other explanations of course remain.

To confirm that the apex oxygen spin-lattice relaxation is indeed of quadrupolar origin, we performed two independent NMR experiments. The first is the application of the double-irradiation technique as described above in the case of plane oxygen. Our second experiment consists in measuring the magnetization recovery of the apex oxygen inner and outer satellites. In general, the recovery depends in a nontrivial way, besides the initial conditions, on magnetic (W) and quadrupolar (W_1, W_2) transition probabilities [32]. To fit the experimental data we performed a Monte Carlo simulation. For a randomly chosen W, W_1, W_2 set, we solved the so-called master rate equation and fitted the resulting multi-exponential magnetization recovery functions simultaneously to the two experimental magnetization recoveries. For each set, the optimal fit delivered its characteristic χ^2 value whose minimum determines the most reliable parameter set (see Fig. 11.6, right).

As in the double-irradiation experiment, we obtained that $W_2, W_1 > W$; so, the apex oxygen relaxation mechanism is predominantly quadrupolar with an unexpectedly small magnetic component. To better understand this interesting result, a detailed theoretical analysis is required.

11.4 Detection of small thermal effects in transition-metal oxides

In the past years, the physics of vortices in novel superconductors has been a matter of very active research [33]. The main focus in thermodynamic experiments on vortex matter has been to study of the first-order melting transition of the "static" vortex lattice, that has been explored in great detail in $YBa_2Cu_3O_{7-\delta}$ [34, 35]. However, depending on the details of the assumed mechanisms to describe the vortex state, a variety of other unconventional phase transitions may exist whose thermodynamics have not yet been explored experimentally [36]. In order to detect the small thermal and magnetic signals associated with vortex physics, we are performing high-precision magnetic and thermal experiments. The high sensitivity of our techniques allows us also to detect other small thermodynamic signals that occur in another physical context.

11.4.1 Lower critical point of the vortex-lattice melting line in $YBa_2Cu_3O_{7-\delta}$

We analyzed our thermal and magnetic data on the discontinuities in magnetization, ΔM, and entropy, ΔS, at the first-order vortex-lattice melting transition in low magnetic fields, as T approaches the critical temperature $T_c = 93.3$ K [37]. Both the magnetic $\Delta M(T)$ data and the $\Delta S(T)$ values from thermal measurements extrapolate to zero around $T/T_c = 0.995$. (T_c was obtained by fitting the corresponding melting field $H_m(T)$ to a power law, $H_m(T) = H_0(1 - T/T_c)^n$). The fact that $\Delta S(T)$ vanishes below the temperature where the melting lines extrapolate to zero might indicate that the first-order character of the phase transition is lost at a lower critical point, that would be located around $\mu_0 H = 80$ mT in our crystals. The large temperature difference between T_c and the temperature where ΔS vanishes (= 450 mK) does not seem to be related in an obvious way to our estimates for the "chemical" full width of the transition to superconductivity (50-100 mK). We therefore conclude that a lower critical point of $H_m(T)$ indeed does exist in our samples, that might be related to the amount and the character of the disorder in the crystals, as has been recently shown for the case of dilute columnar defects [38] .

11.4.2 Investigations on other transition-metal oxides

We performed a number of experiments on other transition-metal oxides using our new high-resolution calorimeter in the temperature range 40-150 K. The apparatus has a resolution in heat of 5 nJ at 77 K. This allows us to start exploring the very challenging magnetic phase diagram of $Bi_2Sr_2CaCu_2O_8$ [36] with a thermal experiment. Unlike in the case of $YBa_2Cu_3O_{7-\delta}$, our first experiments on a 6 mg single crystal did not show any thermal features at the respective vortex-lattice melting transition, presumably because of homogeneity problems with the sample, and due to the fact that the expected thermal signals are of the order of the sensitivity limit of the apparatus.

Another new experimental setup operating in the temperature range 2-40 K is near completion within the framework of a diploma thesis. With this device we will be able to study some unexplored issues in the thermodynamics of certain low-T_c superconductors. Besides the very interesting thermal phenomena that we have already observed in cuprate superconductors [37], we also studied the effect of an oxygen isotope exchange (^{16}O vs. ^{18}O) on the specific heat at the phase transition from the tetragonal low-temperature phase to an

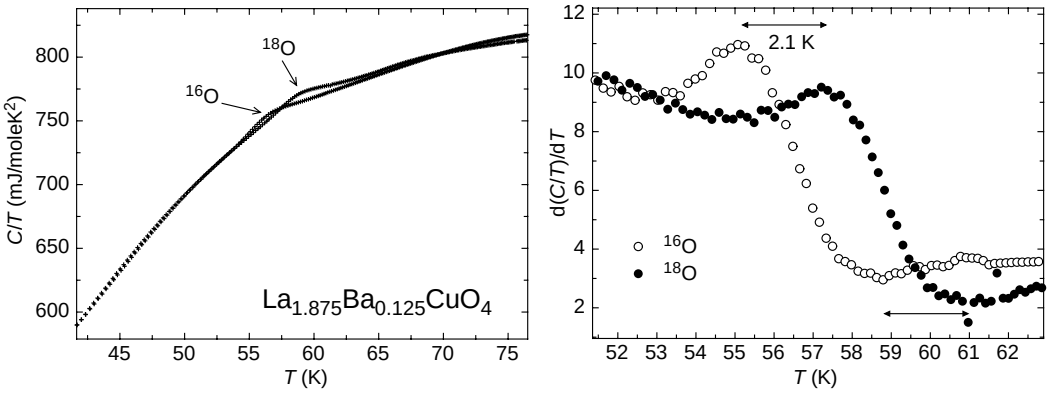

Figure 11.7: *Reduced specific heats C/T of $La_{1.875}Ba_{0.125}CuO_4$ for samples containing the oxygen isotopes ^{16}O and ^{18}O (left figure). The right figure shows the corresponding temperature derivatives to better visualize the observed shift of the transition temperature.*

orthorhombic phase in the non-superconducting compound $La_{1.875}Ba_{0.125}CuO_4$. This transition has been suggested to be closely related to an electronic phase transition or crossover in connection with the formation of charge stripes (see Sec. 11.2.2). In Fig. 11.7 we show the corresponding anomalies in the specific heat that occur at $T = 56.7$ K and 58.8 K for samples containing ^{16}O and ^{18}O, respectively. We believe that the observed discontinuities in the specific heat mainly reflect the signature of the phase transition of the crystal lattice. They do not necessarily contain significant information about an associated change in the electronic structure, the contribution of which is expected to be much smaller than that of the crystal lattice. In analogy to a similar structural phase transition in La_2NiO_4 that is known to be very sensitive to changes in the oxygen sublattice [39], we conclude that the observed oxygen-isotope effect on the transition temperature in $La_{1.875}Ba_{0.125}CuO_4$ can be explained in a natural way by assuming a change in the lattice dynamics of this compound upon isotope exchange, thereby leading to a considerable shift of the observed transition temperature.

11.5 Critical phenomena in the cuprates

Different ordered physical systems, such as fluid, magnetic or superconducting systems, show a singular behavior (described by a power law) of different physical quantities near a critical point [40]. According to their critical behavior these systems are divided into universality classes. Several experiments show that the HTS belong to the 3D XY universality class [41]. During the last two years magnetic torque measurements were performed slightly below and above T_c in magnetic fields $B_a \leq 1.4$ T in order to study critical phenomena in the HTS [42]. In the critical regime of HTS several physical properties are described by a universal scaling function $Q_1^{\pm} dG^{\pm}(z)/dz$, where the scaling variable z depends on the temperature, the applied magnetic field B_a and the field orientation δ [21]. The superscript $\pm$ refers to $T > T_c$ and $T < T_c$, respectively. For instance, the magnetic torque is given by $\tau(T, B_a, \delta) \propto Q_1^{\pm} dG^{\pm}(z)/dz$. As one can see from Fig. 11.8a, where angular-dependent torque measurements performed on different HTS single crystals are displayed, $Q_1^{\pm} dG^{\pm}(z)/dz$ changes its z-dependence drastically upon crossing the critical temperature T_c. The solid lines correspond to the following three limiting behaviors which can be derived analytically [21]: (i) $\lim_{z\to 0-} Q_1^{-} dG^{-}(z)/dz \propto \ln(z)$ $(T < T_c)$, (ii) $\lim_{z\to 0+} Q_1^{+} dG^{+}(z)/dz \propto z$ $(T > T_c)$, (iii) $\lim_{z\to\infty} Q_1^{\pm} dG^{\pm}(z)/dz \propto \sqrt{z}$ $(T \to T_c)$.

For intermediate values of z the scaling function can be experimentally derived by scaling the angular-dependent data recorded at different temperatures [42]. $Q_1^{\pm} dG^{\pm}(z)/dz$ versus z as obtained by this scaling procedure is shown in Fig. 11.8b for various HTS crystals with different anisotropy γ. The scaling functions obtained for the samples investigated deviate systematically with increasing γ from that of $YBa_2Cu_3O_{6.93}$ (Y-123), the sample with the smallest anisotropy. This may be understood in terms of a 3D-2D crossover which leads to non-universal behavior. A quasi-2D feature (the so-called "crossing point" [43]) is present in the scaling function for $z\ \mathrm{sgn}(T/T_c) \sim -0.7$ where a crossover from the $\ln(z)$-dependence to the $\sqrt{z}$-dependence is observed [42].

The $\sin(2\delta)$ signal observed for $T > T_c$ [*c.f.* Fig. 11.8a] yields information about the importance of fluctuations [42]. The amplitude of this signal shows a strong temperature dependence, which is well described by the 3D XY model. The torque signal vanishes at a temperature $T_0 > T_c$ where the $\sin(2\delta)$ amplitude changes its sign. For $T > T_0$ the paramagnetic background of the sample dominates, whereas for $T < T_0$ the fluctuation-induced diamagnetism exceeds the paramagnetic background. Therefore, the quantity $(T_0 - T_c)/T_c$ is a good measure for the importance of superconducting fluctuations. As clearly seen in Fig. 11.8c, fluctuations are more important in the underdoped regime, where γ becomes

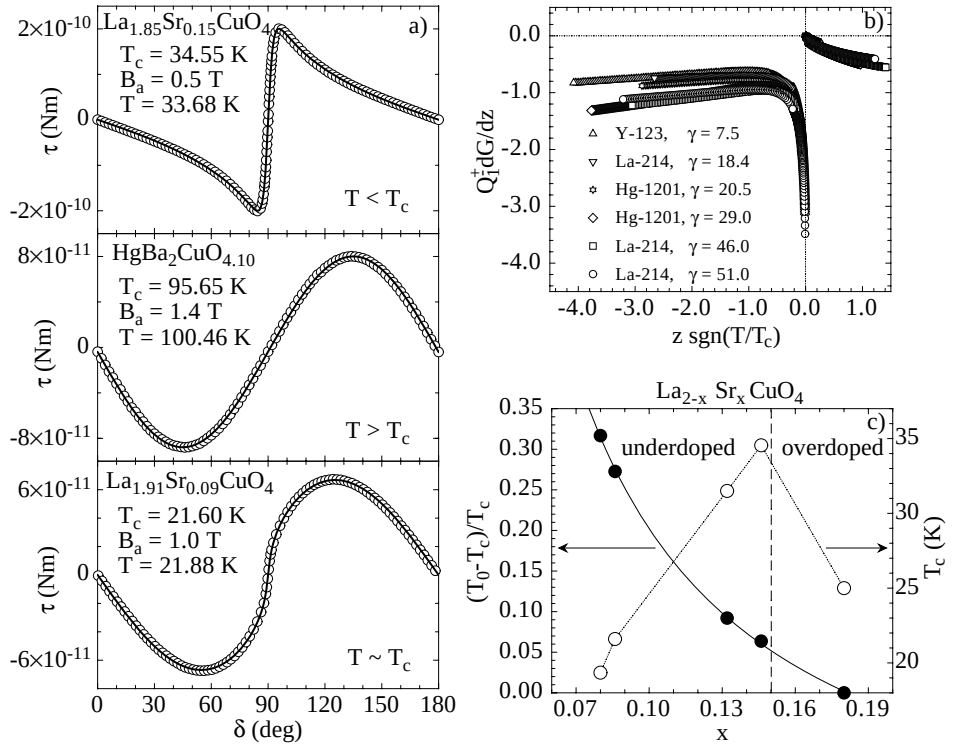

Figure 11.8: *a) Angular-dependent torque measurements performed on HTS at temperatures $T < T_c$, $T > T_c$, $T \sim T_c$. Different angular dependences of the magnetic torque are observed in these three temperature regimes. b) Scaling function $Q_1^{\pm} dG^{\pm}/dz$ as a function of the scaling argument z for various HTS crystals with different anisotropy γ. The scaling function is obtained by scaling angular-dependent data recorded at different temperatures around T_c. The systematic deviations of $Q_1^{\pm} dG^{\pm}/dz$ with increasing γ can be explained by the fact that HTS are in a 3D-2D crossover regime. c) Critical temperature T_c and temperature T_0 (normalized as $(T_0 - T_c)/T_c$) below which the diamagnetic fluctuation signal exceeds the paramagnetic background (see text) as a function of Sr doping x for $La_{2-x}Sr_xCuO_4$ single crystals. Clearly, the importance of fluctuations increases in the underdoped regime, where γ becomes large.*

large. Note that the observation of superconducting fluctuations above T_c clearly demonstrates the existence of preformed pairs. Thus, the physics of underdoped HTS seems to be dominated by fluctuations, and preformed pairs condense into the superconducting state (where they show a macroscopic phase coherence) at T_c.

11.6 Studies of superconductors with low-energy muons

Over the last 12 years μSR has demonstrated to be a unique and extremely powerful microscopic magnetic probe for the study of the complex vortex state in HTS, as well as for investigating local magnetic properties of related magnetically ordered systems. In many cases μSR has provided important information on the microscopic magnetic properties of these materials, which are hardly obtained with other experimental techniques. So far μSR studies have been performed using muons with energies in the MeV range, which require rather thick ($\approx$1mm) samples for the muons to be stopped. Recently, Dr. Elvezio Morenzoni and his collaborators [44, 45] have developed a low-energy (LE) beam of spin polarized muons at the Paul Scherrer Institute (PSI), Switzerland, in order to circumvent this limita-

tion. Very slow muons with kinetic energy of ≈10 eV are obtained from the moderation of high-energy muons in a thin film of a condensed gas. These slow muons of tunable energy between 10 eV and 30 keV can be implanted at very small and controllable depth below the surface of a sample. This allows all the advantages of standard μSR to be obtained in thin samples, near surfaces, and as a function of depth below surfaces (tunable muon energy). The spectrum of possible applications of the novel LE-μSR technique is broad, including magnetic and superconducting thin films and structured materials, quasi two-dimensional magnetic systems, and new materials which can only be prepared in thin film form. It should be pointed out, that at present PSI is the only place in the world where LE-μSR experiments are possible.

Perhaps the most beautiful demonstration of the power of LE-μSR is the recent first direct observation of the spatial variation of the magnetic field (magnetic flux penetration) beneath the surface of a superconductor in the Meissner state [46]. This was achieved by applying a field parallel to the CuO_2 planes of an 700 nm thick epitaxial $YBa_2Cu_3O_{7-\delta}$ film and then measuring the field profile inside the superconductor by implanting LE muons at various depths (15 to 150 nm) by varying the implantation energy of the muons (≈ 3 to 30 KeV). The observed field profile is in excellent accordance with that expected for a thin film from London theory.

In the near future we plan to apply the LE-μSR technique to investigate the complex magnetic phase diagram of $Bi_2Sr_2CaCu_2O_8$, including various vortex phases (vortex solid, vortex glass, vortex liquid). Over the past few years we have investigated these vortex states in the bulk of single-crystal $Bi_2Sr_2CaCu_2O_8$ by means of standard μSR and SANS in great detail. Therefore, it is interesting to explore the vortex structure near the surface in thin films and single crystals with a microscopic probe, such as LE-μSR. In particular, we plan to study vortex-lattice melting and the disorder crossover near the surface of the sample. Is the melting line near the surface and in the bulk the same? Does the melting line change with the thickness of the film? How does the flux-line structure change near the surface of a sample or in a thin film with the magnitude and orientation of the external field? In a further experiment we plan to study the influence of a transport current on the local magnetic flux distribution in a thin HTS film by means of LE-μSR. This allows to investigate the effect of pinning on the flux-line motion on a microscopic scale.

11.7 Medical engineering

In our group, we started to work in the field of medical engineering. The scope of our work is to apply physical measurement techniques to medical problems. In our first project, we focus on ICP (Intracranial Pressure). Since the importance of continuous intracranial pressure measurements for patients after head injury was accepted, intracranial pressure is being used routinely in the management of neurosurgical patients. Several ICP monitoring systems were developed by various research groups. The most common used systems are the fluid filled ventricular catheter (ventricular measurement) and the fiberoptic device with a transducer at the tip (epidural or parenchymal). Although the methods were improved in the last ten years, there is still no highly accurate and reliable method, and there is still a risk of infections and injuries due to the invasion in the brain. There are efforts to develop a less invasive measurement technique to monitor the ICP during several days. In our project, in collaboration with Neurochirurgische Klinik, Ingolstadt, we consider a technique to monitor the ICP indirectly by a strain gauge sensor which measures the extension of the bone due to the pressure. The measurement of the bone extension was already demonstrated by an airspace experiment by NASA Research Laboratory, San Jose (USA). The strain gauge

sensor would be easily implantable and inexpensive. At the moment, we verify the accuracy, handling characteristics, and possible complications in a prospective study.

References

[1] R. von Helmolt *et al.*, Phys. Rev. Lett. **71**, 2331 (1993).

[2] S. Jin *et al.* Science **264**, 413 (1994).

[3] A. P. Ramirez, J. Phys.:Condens. Matter **9**, 8171 (1997).

[4] A. J. Millis, P. B. Littlewood, and B. I. Shraiman, Phys. Rev. Lett. **74**, 5144 (1995).

[5] A. Moreo, S. Yunoki, and E. Dagotto, Science **283**, 2034 (1998).

[6] A. S. Alexandrov, A. M. Bratkovsky, Phys. Rev. Lett. **82**, 141 (1999).

[7] G. M. Zhao *et al.*, cond-mat/9912037.

[8] G. M. Zhao *et al.*, cond-mat/9912355.

[9] J. M. Tranquada *et al.*, Nature (London) **375**, 561 (1995).

[10] H. A. Mook *et al.*, Nature (London) **395**, 580 (1998).

[11] V. J. Emery, S. A. Kivelson, and O. Zachar, Phys. Rev. B**56**, 6120(1997).

[12] G. M. Zhao, K. Ghosh, and R. L. Greene, J. Phys.:Condens. Matter **10**, L737 (1998); G. M. Zhao *et al.*, Phys. Rev. B **59**, 81 (1999).

[13] A. Lanzara *et al.,* J. Phys.: Condens. Matter **11**, L541 (1999).

[14] A. Shengelaya *et al.*, Phys. Rev. Lett. **83**, 5142 (1999)

[15] Ch. Niedermayer *et al.*, Phys. Rev. Lett. **80**, 3843 (1998)

[16] For a review see J.P. Franck, in: *Physical Properties of High Temperature Superconductors IV*, ed. D.M. Ginsberg (World Scientific, Singapore, 1994) (p189-293).

[17] G.M. Zhao *et al.*, J. Phys.: Condens. Matter **10**, 9055 (1998).

[18] J. Hofer *et al.*, preprint (cond-mat/9912493).

[19] M. Willemin *et al.*, J. Appl. Phys. **83**, 1163 (1998).

[20] D.E. Farrell *et al.*, Phys. Rev. Lett. **61**, 2805 (1988).

[21] T. Schneider *et al.*, Eur. Phys. J. B **3**, 413 (1998).

[22] A.S. Alexandrov and N.F. Mott, *Polarons and Bipolarons* (World Scientific, Singapore, 1995).

[23] K.A. Müller *et al.*, J. Phys.: Condens. Matter **10**, L291 (1998).

[24] A. Shengelaya *et al.*, submitted for publication to Phys. Rev. B

[25] F.C. Zhang and T.M. Rice, Phys. Rev. B **37**, 3759 (1988).

[26] V.J. Emery and G. Reiter, Phys. Rev. B **38**, 11938 (1988); J.P. Lu, Q. Si, J.H. Kim, and K. Levine, Phys. Rev. Lett. **65**, 2466 (1990).

[27] A. Suter, M. Mali, J. Roos, and D. Brinkmann, J. Magn. Reson. **143**, 266 (2000).

[28] A. Suter, M. Mali, J. Roos, and D. Brinkmann, (cond-mat/9907043).

[29] V.J. Emery and S.A. Kivelson, Physica C **235–240**, 189 (1994); J. Ranninger and J.M. Robin, Phys. Rev. B **53**, 15657 (1996).

[30] A.S. Alexandrov and N.F. Mott, Rep. Prog. Phys. **57**, 1197 (1994).

[31] F. Raffa *et al.*, Phys. Rev. B **60**, 3636 (1999).

[32] A. Suter, M. Mali, J. Roos, and D. Brinkmann, J. Phys. Condens. Matter **10**, 5977 (1998).

[33] G. Blatter *et al.*, Rev. Mod. Phys. **66**, 1125 (1994) .

[34] U. Welp *et al.*, Phys. Rev. Lett. **76**, 4809 (1996).

[35] A. Schilling *et al.*, Nature **382**, 791 (1996).

[36] M. F. Goffman *et al.*, Phys. Rev. B **57**, 3663 (1998).

[37] A. Schilling *et al.*, Phys. Rev. B **61**, 3592 (2000).

[38] W. K. Kwok *et al.*, to appear in Phys. Rev.

[39] J. Rodriguez-Carvajal *et al.*, Phys. Rev. B **38**, 7148 (1988).

[40] For an overview see *e.g.* Shang-Keng Ma, *Modern Theory of Critical Phenomena*, Frontiers in Physics **46** (W.A. Benjamin, Inc., Reading, Massachusettes, 1976).

[41] S. Kamal *et al.*, Phys. Rev. B **58**, R8933 (1998); V. Pasler *et al.*, Phys. Rev. Lett. **81**, 1094 (1998).

[42] J. Hofer *et al.*, Phys. Rev. B **60**, 1332 (1999); J. Hofer *et al.*, preprint (cond-mat/9912052).

[43] P.H. Kes *et al.*, Phys. Rev. Lett. **67**, 2383 (1991).

[44] E. Morenzoni *et al.*, J. Appl. Phys. **81**, 3340 (1997).

[45] E. Morenzoni, *Physics and applications of low energy muons*, in Muon Science, S.L. Lee *et al.* Eds., IOP Publishing (1999).

[46] T.J. Jackson *et al.*, to appear in Phys. Rev. Lett. (2000).